Dynamic Multiple-Period Reconfiguration of Real-Time Scheduling Based on Timed DES Supervisory Control

ARTICLE *in* IEEE TRANSACTIONS ON INDUSTRIAL INFORMATICS · FEBRUARY 2016

Impact Factor: 8.79 · DOI: 10.1109/TII.2015.2500161

3 AUTHORS:

Xi Wang

Xidian University

3 PUBLICATIONS **12** CITATIONS

SEE PROFILE

Zhiwu Li

Xidian University

223 PUBLICATIONS **3,662** CITATIONS

SEE PROFILE

Walter Wonham

University of Toronto

246 PUBLICATIONS **19,952** CITATIONS

SEE PROFILE

Dynamic Multiple-Period Reconfiguration of Real-Time Scheduling Based on Timed DES Supervisory Control

Xi Wang, ZhiWu Li, *Senior Member, IEEE*, and W. M. Wonham, *Life Fellow, IEEE*

***Abstract*—Based on the supervisory control theory (SCT) of timed discrete-event systems (TDES), this study presents a dynamic reconfiguration technique for real-time scheduling of real-time systems running on uni-processors. A new formalism is developed to assign periodic tasks with multiple-periods. By implementing SCT, a real-time system (RTS) is dynamically reconfigured when its initial safe execution sequence set is empty. During the reconfiguration process, based on the multiple-periods, the supervisor proposes different safe execution sequences. Two real-world examples illustrate that the presented approach provides an increased number of safe execution sequences as compared to the earliest-deadline-first (EDF) scheduling algorithm.**

***Index Terms*—Real-time system, timed discrete-event system, supervisory control, dynamic reconfiguration, non-preemptive scheduling.**

I. Introduction

In [1], Liu and Layand define a periodic task model with a deadline equal to its period, which we refer to as the Liu-Layand (LL) model. Thereafter, Nassor and Bres propose a new task model in [2], with a deadline less than or equal to its period, which we refer to as the Nassor-Bres (NB) model. Currently, the most widely-used scheduling algorithms for hard periodic real-time systems (RTS) running on a uni-processor are fixed priority (FP) scheduling and earliest-deadline-first (EDF) scheduling algorithms [1]. Moreover, an RTS can be scheduled in a preemptive or non-preemptive mode [3], [4]. In real-time scheduling theory, these widely applied algorithms provide at most one schedulable sequence for an RTS to meet the hard deadlines. For non-preemptive scheduling of an RTS that executes the NB model tasks, Chen and Wonham [6] propose a timed discrete-event system (TDES)-based task model, which we refer to as the Chen-Wonham (CW) model, and a real-time scheduling technique. Based on supervisory control theory (SCT), all safe execution sequences are generated by the TDES supervisor, from which the user chooses preferred sequences to schedule the RTS. The RTS is claimed to be non-schedulable if the supervisor is empty. Based on the LL model and SCT, a priority-based and preemptive real-time scheduling policy and a task model, which we refer to as the Janarthanan-Gohari-Saffar (JGS) model, are proposed by Janarthanan et al. in [7]. The work in [6] and [7] is a significant improvement over real-time scheduling. However, the authors did not reconfigure the system in case of non-schedulability.

In [8]–[11], an elastic period task model is proposed to handle the overload of an RTS by decreasing the task processor utilization. Moreover, the supremal controller found by SCT provides the RTS with all the safe execution sequences [6]. Building on the two latter studies, we present a new modeling technique to endow the real-time tasks represented by the CW and JGS models with multiple-periods. To handle the overload of an RTS, SCT is utilized to find all the possible solutions based on different periods of each task. For each solution, all the safe execution sequences are provided.

Dynamic reconfiguration in the present study consists of two steps: 1) the initial model of each task is assigned with the shortest period (the highest processor utilization), and by utilizing SCT, all the RTS' safe execution sequences (if any) are found; 2) for the purpose of reconfiguring the RTS in case of non-schedulability, this study reconfigures the RTS' composite task model by assigning to the tasks multiple-periods. The multiple-period provides multiple processor utilization for each task. Thereafter, a processor utilization interval for the RTS is obtained. SCT is utilized again to find all the safe execution sequences (possible reconfiguration scenarios) in the predefined processor utilization interval. If the supervisor is still empty, we claim that the RTS is non-schedulable. Two real-world examples are implemented in this study. The results illustrate that, in the dynamic reconfiguration approach, the presented method finds a set of safe execution sequences.

The rest of this paper is structured as follows. The state of the art is reviewed in Section II. Section III presents the terminology used throughout the paper. The multiple-period TDES model for RTS is defined in Section IV. Section V reports methodologies of supervisory control and reconfiguration of RTS. A real-world example is implemented in Section VI to verify the supervisory control and reconfiguration. Further

This work was supported in part by the National Natural Science Foundation of China under Grant No. 61374068 and the Science and Technology Development Fund, MSAR, under Grant No. 066/2013/A2 (Corresponding author: ZhiWu Li).

X. Wang is with the School of Electro-Mechanical Engineering, Xidian University, Xi'an 710071, China, and also with the Systems Control Group, Department of Electrical and Computer Engineering, University of Toronto, Toronto, ON M5S 3G4, Canada (e-mail: wanggkingg@gmail.com).

Z. W. Li is with the Faculty of Information Technology, Macau University of Science and Technology, Taipa, Macau, and also with the School of Electro-Mechanical Engineering, Xidian University, Xi'an 710071, China (e-mail: zhwli@xidian.edu.cn).

W. M. Wonham is with Department of Electrical and Computer Engineering, University of Toronto, Toronto, ON M5S 3G4, Canada (e-mail: wonham@control.utoronto.ca).

relevant issues are discussed in Section VII. Conclusions are provided in Section VIII.

II. State of the Art

In a periodic RTS, a permanent overload condition occurs if the processor utilization is greater than one [12]. In this case, the RTS needs to be reconfigured [13]. In recent years several academic and industrial studies [14]–[16] have addressed the dynamic reconfiguration of RTS. These approaches can be divided into two categories: manual, applied by users [17], and automatic, applied by intelligent control agents [18]. The most widely used overload management approaches are: elastic scheduling [8]–[11] and job skipping [19]. In real-time scheduling, effective solutions for reconfiguration based on sensitivity approach of worst-case execution times (WCET), deadlines, and periods of tasks are reviewed in [20]. These solutions are utilized to reconfigure the RTS scheduled by FP real-time scheduling [21]. There is no reconfiguration result [22] based on the sensitivity approach to reconfigure the tasks' periods for dynamic-priority real-time scheduling [20]. Based on SCT, this study presents a new dynamic reconfiguration technique to reconfigure the RTS when they are claimed to be non-schedulable under the approaches in [6] or [7]. Unlike traditional real-time scheduling and reconfiguration via the calculation of processor utilization, processor demand [23], and on-line monitoring to provide one safe execution sequence, an off-line technique is presented: in a predefined processor utilization interval, based on SCT, all the possible reconfiguration scenarios are found.

III. Concepts and Terminology

A. Preliminaries on TDES

In the language-based Ramadge-Wonham (RW) framework [24], [25], a finite discrete-event system (DES) is represented by a state machine $\mathbf{G} = (Q, \Sigma, \delta, q_0, Q_m)$, where Q is the state set, Σ is the event set, δ: $Q \times \Sigma \to Q$ is the (partial) state transition function, q_0 is the *initial* state, and Q_m is the *marker* state set satisfying $Q_m \subseteq Q$. Let Σ^+ (resp., ϵ) denote the set of all finite sequences over Σ (resp., empty string). We have $\Sigma^* = \Sigma^+ \cup \{\epsilon\}$. A plant and a specification are represented by $\mathbf{G}$ and $\mathbf{S}$, respectively. In [26], by adjoining to the RW framework time bounds on the transitions, $\mathbf{G}$ starts from an (untimed) activity transition graph (ATG) $\mathbf{G_{act}} = (A, \Sigma_{act}, \delta_{act}, a_0, A_m)$ with $\Sigma := \Sigma_{act} \dot\cup \{tick\}$. The elements of the activity set A are "activities", denoted by a. Σ_{act} is partitioned into two subsets, $\Sigma_{act} = \Sigma_{spe} \dot\cup \Sigma_{rem}$, where Σ_{spe} (resp. Σ_{rem}) is the *prospective* (resp. *remote*) event set with *finite* (resp. *infinite*) upper time bounds [25]. By defining the *timer interval* for σ, represented by T_σ, to be $[0, u_\sigma]$ or $[0, l_\sigma]$ for $\sigma \in \Sigma_{spe}$ and $\sigma \in \Sigma_{rem}$, respectively, the *initial* state is $q_0 := (a_0, \{t_{\sigma 0} | \sigma \in \Sigma_{act}\})$, where $t_{\sigma 0}$ equals u_σ or l_σ for a *prospective* or *remote* state, respectively. The *marker* state set is $Q_m \subseteq A_m \times \prod\{T_\sigma | \sigma \in \Sigma_{act}\}$. Thus a TDES is represented by $\mathbf{G} = (Q, \Sigma, \delta, q_0, Q_m)$. An event $\sigma \in \Sigma_{act}$ is *enabled* at q if $\delta_{act}(a, \sigma)$ is defined, written $\delta_{act}(a, \sigma)!$; it is *eligible* if its transition $\delta(q, \sigma)$ is also defined, i.e., $\delta(q, \sigma)!$. The *closed behavior* of $\mathbf{G}$ is the language $L(\mathbf{G}) := \{s \in \Sigma^* | \delta(q_0, s)!\}$. In addition, the *marked behavior* of $\mathbf{G}$ is $L_m(\mathbf{G}) := \{s \in L(\mathbf{G}) | \delta(q_0, s) \in Q_m\}$. $\mathbf{G}$ is *non-blocking* if $L_m(\mathbf{G})$ satisfies $\overline{L_m(\mathbf{G})} = L(\mathbf{G})$, where $\overline{L_m(\mathbf{G})}$ is the *(prefix) closure* of $L(\mathbf{G})$. In a TDES plant $\mathbf{G}$, the eligible event set $Elig_{\mathbf{G}}(s) \subseteq \Sigma$ at a state q corresponding to a string $s \in L(\mathbf{G})$ is defined by $Elig_{\mathbf{G}}(s) := \{\sigma \in \Sigma | s\sigma \in L(\mathbf{G})\}$. For an arbitrary language $K \subseteq L(\mathbf{G})$, let $s \in \overline{K}$, $Elig_K(s) := \{\sigma \in \Sigma | s\sigma \in \overline{K}\}$. The set of all controllable sublanguages of K is denoted by $\mathcal{C}(K)$; this family is nonempty (the empty set belongs) and is closed under arbitrary set unions. Hence, a unique supremal (i.e., largest) element exists, and is denoted by sup$\mathcal{C}(K)$. Considering a specification language $E \subseteq \Sigma^*$, there exists an optimal *monolithic supervisor* $\mathbf{S}$. Its closed behavior is $L(\mathbf{S}) = \overline{L_m(\mathbf{S})}$, where $L_m(\mathbf{S})$ is the marked behavior represented by $L_m(\mathbf{S}) =$sup$\mathcal{C}(E \cap L_m(\mathbf{G})) \subseteq L_m(\mathbf{G})$.

B. System Model

Suppose that a periodic RTS $\mathbb{S}$ processes n tasks, i.e., $\mathbb{S} = \{\tau_1, \tau_2, \ldots, \tau_n\}$, $i \in \mathbf{n}$. Assume also that this set contains at least one task with a *multiple-period*, namely one having a lower and upper (non-negative integral time) bound. The execution model of such a system is a set of tasks processed in a uni-processor, in which a task τ_i is described by $\tau_i = (R_i, C_i, D_i, T_i)$ with a release time R_i; a WCET C_i; a hard deadline D_i; and a multiple-period T_i. An RTS is a *synchronous* system [23] in case all the processed tasks are released at the same time, namely $R_i = 0$. In this research the RTS is synchronous. A deadline is *hard* if its violation is unacceptable. A multiple-period is a period set containing several possible periods: the lower bound (i.e., shortest one) is represented by $T_{i_{min}}$, and the upper bound (i.e., longest one) is represented by $T_{i_{max}}$. Thus, we have $T_i = [T_{i_{min}}, T_{i_{max}}]$.

During the real-time scheduling process, for task τ_i, only one period T satisfying $T_{i_{min}} \leq T \leq T_{i_{max}}$ is selected in each scheduling period. The processor utilization U_i of task τ_i is calculated by $U_i = C_i/T$. The total processor utilization of $\mathbb{S}$ is $U_{\mathbb{S}} = \sum_{i=1}^{n} U_i$. An RTS $\mathbb{S}$ is not schedulable in case $U_{\mathbb{S}} > 1$ [12].

Task τ_i consists of an infinite sequence of jobs $J_{i,j} = (r_{i,j}, C_i, d_{i,j}, p_{i,j})$ repeated periodically. The *absolute deadline* $d_{i,j}$ denotes the global clock time at which the execution of $J_{i,j}$ must be completed. Similarly, we define the *absolute release time* (resp. *period*) $r_{i,j}$ (resp. $p_{i,j}$) to mean the global clock time at which τ_i must be released (resp. start the next period). The subscript "i, j" of $J_{i,j}$ represents the j-th execution of task τ_i. For each j, $J_{i,j}$ requests the processor at global clock time $r_{i,j}$. Moreover, the execution of $J_{i,j}$ takes C_i ticks, which must be completed no later than $d_{i,j}$. The absolute deadline $d_{i,j}$ occurs no later than the absolute period $p_{i,j}$. The EDF scheduling algorithm [1] assigns the priority of each job based on the absolute deadlines: the earlier the deadline, the higher is the job's priority. The EDF scheduling algorithm can be utilized to schedule RTS. At each time unit, the job with the highest priority enters the processor. If the execution of a job is allowed to be preempted by other jobs before its execution finishes, the scheduling is preemptive; otherwise, it is non-preemptive.

IV. TDES Model for Real-Time Systems

A. CW Model

The CW model [6] represents a real-time periodic task $\tau_i = (R_i, C_i, D_i, T_i)$, $i \in \mathbf{n}$, with $D_i \leq T_i$, by a TDES $\mathbf{G}_i = (Q_i, \Sigma_i, \delta_i, q_{0i}, Q_{mi})$. As depicted in Fig. 1, the corresponding ATG part is $\mathbf{G_{act}} = (A_i, \Sigma_{acti}, \delta_{acti}, a_{0i}, A_{mi})$ with

- $A_i = \{Y_i, I_i, W_i\}$,
- $\Sigma_{acti} = \{\gamma_i, \alpha_i, \beta_i\}$,
- $\delta_{acti} : A_{acti} \times \Sigma_{acti} \rightarrow A_{acti}$ with
  - $\delta_{acti}(Y_i, \gamma_i) = I_i$,
  - $\delta_{acti}(I_i, \alpha_i) = W_i$, and
  - $\delta_{acti}(W_i, \beta_i) = Y_i$.
- $a_{0i} = Y_i$, and
- $A_{mi} = \{Y_i\}$.

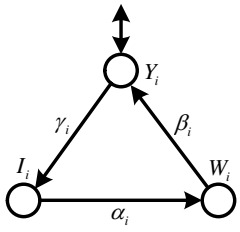

Fig. 1: ATG of a real-time task.

States Y_i, I_i, and W_i represent that task τ_i is at states *delay*, *idle*, and *work*, respectively. The events in the alphabet Σ_i are

- γ_i: the event that τ_i is released,
- α_i: the execution of τ_i is started, and
- β_i: the execution of τ_i is finished.

Event α_i is controllable and events γ_i and β_i are uncontrollable. Moreover, all the events in Σ_{acti} are forcible. Suppose that, after enabling, events γ_i, α_i, and β_i should wait for t_{γ_i}, t_{α_i}, and t_{β_i} ticks, respectively, until they are eligible to occur. Thus, t_{α_i} is the time at which τ_i starts its execution. Furthermore, in the CW model, $t_{\beta_i} = C_i$. A CW model has the following two features: 1) γ_i signals that after $r_{i,1}$, τ_i will release at every T_i ticks periodically; and 2) β_i must occur before τ_i is released again. The time interval between the occurrences of events β_i and γ_i is the remaining time of the current period, which decreases along with the increase of t_{α_i}. Hence, in two adjacent periods, the values of t_{γ_i} could be different. Formally,

- γ_i has time bounds $\begin{cases} [0,0], \\ \quad \text{if } \tau_i \text{ releases at } r_{1,1} \\ [T_i - t_{\alpha_i} - t_{\beta_i}, T_i - t_{\alpha_i} - t_{\beta_i}], \\ \quad \text{if } (\forall j > 1)\ \tau_i \text{ releases at } r_{i,j} \end{cases}$,
- α_i has time bounds $[0, D_i - t_{\beta_i}]$, and
- β_i has time bounds $[t_{\beta_i}, t_{\beta_i}]$.

B. JGS Model

Another TDES real-time task model, the JGS model proposed in [7], can be utilized to preemptively schedule periodic tasks τ_i satisfying $D_i = T_i$. The scheduling is priority-based. The general TDES models for the WCET and the period of each task are represented by the two TDES generators shown in Figs. 2 and 3, respectively, in which $\Sigma = \Sigma_1 \cup \Sigma_2 \cup \cdots \cup \Sigma_n$, and $\Sigma^t = \Sigma \cup \{t\}$. The event set Σ_i for τ_i is composed of a_i, the arrival of task τ_i; c_i, the execution of task τ_i; and e_i, the execution of the last time unit of task τ_i. Event a_i is uncontrollable while events c_i and e_i are controllable. Moreover, all the events in the alphabet Σ_i are forcible.

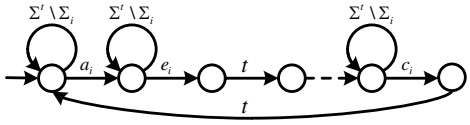

Fig. 2: JGS WCET model.

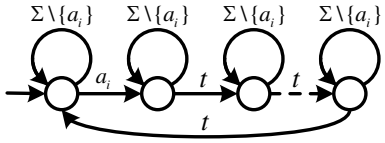

Fig. 3: JGS period model.

C. Comparison between CW and JGS Models

Several differences between the CW and JGS models are shown in Table I, in which Y and N represent "yes" and "no", respectively.

TABLE I: CW model v.s. JGS model

Model	$D \leq T$	priority	preemption
CW	Y	N	N
JGS	N	Y	Y

Both CW and JGS models have their advantages and disadvantages. Thus they can be utilized to model different RTS. The CW model can be utilized to model an RTS executing a set of periodic tasks with deadlines less than or equal to their corresponding periods. However, priority-based scheduling and preemptive scheduling cannot be accommodated by the CW model. On the contrary, the JGS model can only be utilized to model an RTS executing a set of tasks with deadlines equal to their periods. Moreover, in the JGS model, priority-based scheduling and preemptive scheduling of real-time tasks are addressed. Users can choose different models to solve different real-time scheduling problems.

D. TDES Model for Multiple-Period Tasks

The elastic task model in [8]–[11] assigns a lower and an upper period bound for each task to dynamically reconfigure an RTS. At each time, the reconfiguration of each task's period is assigned a value between the two bounds $T_{i_{min}}$ and $T_{i_{max}}$. Consequently, the processor utilization U_i of an elastic periodic task has a lower bound $U_{i_{min}}$ and an upper bound $U_{i_{max}}$. Formally, we have

$$U_i = [U_{i_{min}}, U_{i_{max}}]$$

with $U_{i_{min}} = C_i/T_{i_{max}}$ and $U_{i_{max}} = C_i/T_{i_{min}}$. The system processor utilization is

$$U_{\mathbb{S}} = [U_{min}, U_{max}]$$

with $U_{min} = \sum_{i=1}^{n} U_{i_{min}}$ and $U_{max} = \sum_{i=1}^{n} U_{i_{max}}$. In the interval $[U_{min}, U_{max}]$, there may exist multiple safe execution sequences (reconfiguration scenarios) that correspond to different processor utilizations. Moreover, SCT [25] is utilized to find the supremal controllable sublanguages, i.e., it is possible to provide multiple reconfiguration scenarios for each task. Building on the elastic task model and SCT, we present a new model that provides all the possible periods for each task; the supervisor provides all the safe execution sequences (possible reconfiguration scenarios) simultaneously. Users choose any scenario to reconfigure the RTS dynamically.

A regular periodic task with a fixed period is considered as a multiple-period task τ_i with $T_{i_{min}} = T_{i_{max}}$. With a regular task, the reconfiguration of its period would affect its utilization, which is not allowed. On the other hand, SCT is utilized to provide all the possible scheduling paths based on different periods (utilizations).

1) Multiple-period CW (MCW) model:

In this study, the MCW model is depicted in Fig. 4, in which y_0 is the *initial* state, and $\{y_{min}, y_{min+1}, \ldots, y_{max-1}, y_0\}$ is the *marker* state set. Each marker state represents that τ_i has finished the current execution of $J_{i,j}$ and is ready for the release of $J_{i,j+1}$. State y_0 represents that job $J_{i,j}$ finishes its operation at $T_{i_{max}}$ or has never been invoked. States y_{min}, y_{min+1}, and y_{max-1} represent that job $J_{i,j}$ finishes its operation at times $T_{i_{min}}$, $T_{i_{min+1}}$, and $T_{i_{max-1}}$, respectively.

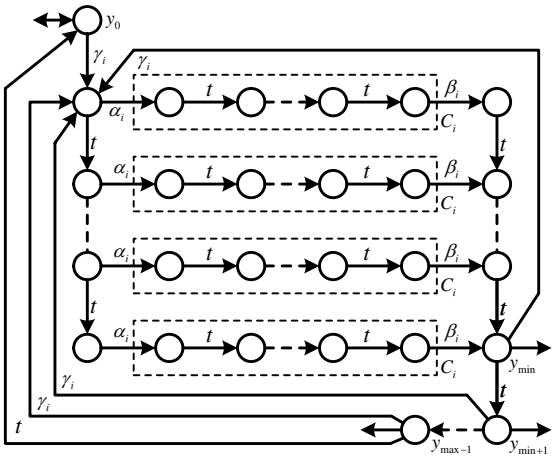

Fig. 4: General TTG model for MCW tasks.

On the occurrence of α_i, τ_i starts the processing of the current job. After event *tick* occurs C_i times, the execution of τ_i is completed. The next occurrence of event γ_i drives τ_i into the next execution period. Formally,

- γ_i has time bounds $\begin{cases} [0,0], \\ \quad \text{if } \tau_i \text{ releases at } r_{i,1} \\ [T_{i_{min}} - t_{\alpha_i} - t_{\beta_i}, T_{i_{max}} - t_{\alpha_i} - t_{\beta_i}], \\ \quad \text{if } (\forall j > 1)\ \tau_i \text{ releases at } r_{i,j} \end{cases}$,
- α_i has time bounds $[0,\ \min\{D_i, T_{i_{min}}\} - t_{\beta_i}]$, and
- β_i has time bounds $[t_{\beta_i}, t_{\beta_i}]$.

Remarks:

1. Initially, a task with $T_i = T_{i_{min}}$ plays the role of the task proposed in [6], i.e., task τ_i always stays at the highest processor utilization. If the RTS is non-schedulable, the multiple-period model with $T_i = [T_{i_{min}}, T_{i_{max}}]$ is utilized to provide all the possibilities to compress the processor utilization.

2. The remaining time between β_i and γ_i equals 0 if 1) $D_i = T_i$ and 2) α_i occurs at time $D_i - t_\beta$. As a result, the occurrence of β_i may lead the TDES model to state y_0 directly. Suppose that we have a task $\tau_i = (0, 2, 5, [3, 5])$. The corresponding TTG model $\mathbf{G}_i$ is illustrated in Fig. 5. All the possible processor utilizations of τ_i are $2/3$, $2/4$, and $2/5$.

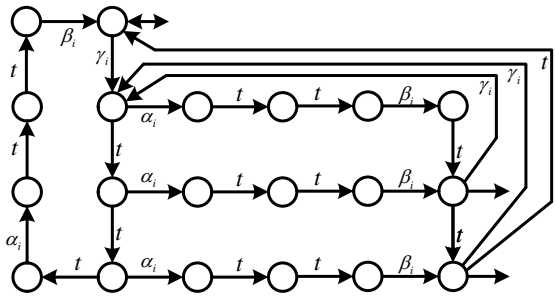

Fig. 5: Multiple-period TDES $\mathbf{G}_i$.

3. The time bounds $[T_{i_{min}} - t_{\alpha_i} - t_{\beta_i}, T_{i_{max}} - t_{\alpha_i} - t_{\beta_i}]$ for event γ_i for $r_{i,j}$ with $j \geq 1$ are dynamic, which decreases along with the increase of t_{α_i}.

2) Multiple-period JGS (MJGS) model:

In order to assign a multiple-period to a JGS model, we need to define marker states. Consequently, the initial states are revised, i.e., they are also assigned to be marker states. The new models for WCET and multiple-period are depicted in Figs. 6 and 7, respectively. In Fig. 7, we have that y_0 is the initial state; and $\{T_{i_{min}}, y_{i_{min}+1}, \ldots, y_{i_{min}-1}, y_0\}$ is the marker state set. Each marker state represents that τ_i has finished the current execution of $J_{i,j}$ and is ready for the release of $J_{i,j+1}$. State y_0 represents that job $J_{i,j}$ finishes its operation at $T_{i_{max}}$ or has never been invoked. States y_{min}, y_{min+1}, and y_{max-1} represent that job $J_{i,j}$ finishes its operation at times $T_{i_{min}}$, $T_{i_{min+1}}$, and $T_{i_{max-1}}$, respectively. The following transition rule represents the new arrival of τ_i:

$$(q \in \{T_{i_{min}}, y_{i_{min}+1}, \ldots, y_{i_{min}-1}, y_0\}) \Rightarrow \delta(q, a_i) = 0.$$

Example.

Let $\tau_x = (0, 1, [2, 3], [2, 3])$ be a periodic task. The WCET and multiple-period models of τ_x are shown in Fig. 8. The processor utilization of τ_x could be $1/2$ or $1/3$.

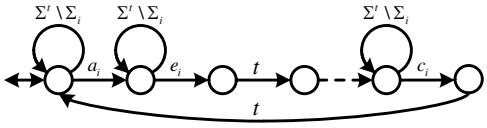

Fig. 6: Revised WCET of JGS model.

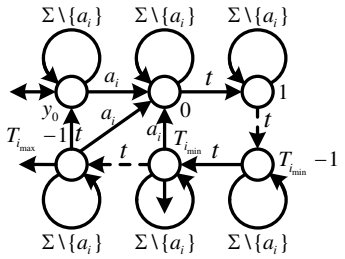

Fig. 7: Multiple-period of a JGS model.

E. Task Creation and Editing in TTCT

The TDES synthesis procedure TTCT [1] is a software package to create an RTS as the composite model [6] of multiple-period TDES models and to execute further operations. All the operations and the generated files are recorded in an annotated file **MAKEIT.TXT**. In this study, a task with a superscript "l" (resp. "u") represents that it possesses the lower (resp. upper) period bound; the corresponding task name in TTCT is prefixed by an L (resp. U).

1) Task creation for MCW model:

The tasks τ_1, τ_2, and τ_3 listed in Table II are created by TTCT. The types "M" and "F" in Table II denote that the corresponding task possesses multiple-period or fixed-period (as in a CW model), respectively.

TABLE II: Parameters of MCW Tasks

task	type	TTCT	R	C	D	T
τ_1	M	TASK1	0	1	4	5
τ_2	M	TASK2	0	2	6	[4, 6]
τ_2^l	F	LTASK2	0	2	4	4
τ_2^u	F	UTASK2	0	2	6	6
τ_3^l	F	LTASK3	0	2	3	3
τ_3	M	TASK3	0	2	5	[3, 5]
τ_3^u	F	UTASK3	0	2	5	5

2) Task creation for MJGS model:

The WCET and periods of tasks τ_a, τ_a^l, and τ_b listed in Table III are created by TTCT. The WCET of τ_a (τ_a^l) and τ_b are named by CA and CB, respectively. The periods of τ_a, τ_a^l, and τ_b are named PA, LPA, and PB, respectively.

F. TDES RTS Model

The composite model of an RTS is generated by the synchronous product of all the tasks [6], [25].

[1]http://www.control.utoronto.ca/DES

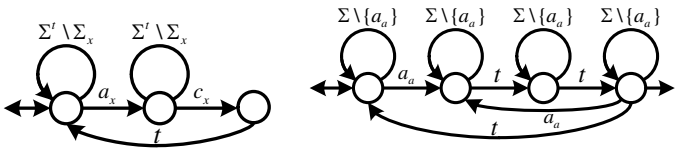

(a) WCET (b) Multiple-period

Fig. 8: TDES models of τ_x.

TABLE III: Parameters of MJGS Tasks

task	type	R	C	D	T
τ_a	M	0	1	[2, 3]	[2, 3]
τ_a^l	F	0	1	2	2
τ_b	F	0	2	3	3

1) MCW RTS generation:

Suppose that tasks τ_1 and τ_2 are running in RTS $\mathbb{S}^0$. We generate $\mathbb{S}^0$ by the following TTCT procedures (all the **sync** operations in the original **MAKEIT** file were reported with the message "Blocked_events = None", eliminated here for readability):

SYS0 = **sync** (TASK1, TASK2) (425, 644)

where "(425, 644)" denotes that $\mathbb{S}^0$, represented by SYS0, has 425 states and 644 transitions. Suppose that another RTS $\mathbb{S}^1$, represented by SYS1, contains τ_1, τ_2, and τ_3. It is generated based on $\mathbb{S}^0$ as follows.

SYS1 = **sync** (SYS0, TASK3) (8500, 16367)

The composite task model of traditional periodic RTS is generated by the technique proposed in [6]. In this study, by choosing the periodic tasks with the lower (resp. upper) bound of periods, we generate $\mathbb{S}_l^0$ (LSYS0), $\mathbb{S}_l^1$ (LSYS1), and $\mathbb{S}_u^1$ (USYS1) as follows. They are the counterparts of $\mathbb{S}^0$ and $\mathbb{S}^1$ with fixed-periods.

LSYS0 = **sync** (TASK1, LTASK2) (255, 364)

LSYS1 = **sync** (LSYS0, LTASK3) (2550, 4475)

USYS1 = **sync** (TASK1, UTASK2) (425, 610)

USYS1 = **sync** (USYS1, UTASK3) (1750, 3064)

Finally, the five generated MCW RTS are listed in Table IV; they will be utilized in the supervisory control and evaluation of the closed behavior of the controlled RTS.

TABLE IV: Parameters of MCW Systems

system	type	TTCT	tasks
$\mathbb{S}^0$	M	SYS0	τ_1, τ_2
$\mathbb{S}^1$	M	SYS1	τ_1, τ_2, τ_3
$\mathbb{S}_l^0$	F	LSYS0	τ_1, τ_2^l
$\mathbb{S}_l^1$	F	LSYS1	τ_1, τ_2^l, τ_3^l
$\mathbb{S}_u^1$	F	USYS1	τ_1, τ_2^u, τ_3^u

2) MJGS RTS generation:

The MJGS model for an RTS $\mathbb{S}_l^J$ executing τ_a^l and τ_b is represented by a generator LJ that is generated as follows.

SYS = **sync** (CA, CB) (13, 34)

LP = **sync** (LPA, PB) (12, 61)

LJ = **sync** (SYS, LP) (89, 155)

The MJGS model $\mathbb{S}^J$ for an RTS executing τ_a and τ_b, represented by J, is generated in a similar way, i.e.,

P = **sync** (PA, PB) (16, 85)

J = **sync** (SYS, P) (124, 228)

V. Supervisory Control of Dynamic Reconfigurable Multiple-Period RTS

The event controllability and the supervisory control in this study follow the principles proposed in [6], [7], and [25].

A. General Specification for MCW Model

Instead of utilizing the method proposed in [6] to dynamically revise the specifications, a general specification $\mathbf{S}$ with

$$L(\mathbf{S}) = L(\mathbf{S}_1)||L(\mathbf{S}_2)||\cdots||L(\mathbf{S}_n)$$

is defined with event set $\Sigma = \bigcup_{1\leq i\leq n}\Sigma_i$, the union of the event sets of all the potential tasks which may be called by the processor. Let $L(\mathbf{S}) = E \subseteq \Sigma^*$. Moreover, $L_m(\mathbf{G}) \subseteq \Sigma^*$ is always satisfied. Hence, by Theorem 1 (Theorem 3.5.2 in [25]), K can be found by the procedure **supcon**.

Theorem 1: [25] Let $E \subseteq \Sigma^*$ and let $K = sup\mathcal{C}(E \cap L_m(\mathbf{G}))$. If $K \neq \emptyset$ there exists a marking nonblocking supervisory control (MNSC) for $\mathbf{G}$ such that $L_m(V/\mathbf{G}) = K$.

In order to use SCT to schedule the RTS non-preemptively, the specifications are defined to ensure that after the occurrence of α_i, no other event α_j with $j \neq i$ can occur to preempt it. Hence, the TDES model of specification $\mathbf{S}_i$ for task τ_i is illustrated in Fig. 9(a), in which α_j and β_j with $j \neq i$ represent events α and β for any other task, respectively. The symbol $*$ represents the other events in Σ. The specifications for $\mathbf{G}_1$, $\mathbf{G}_2$, and $\mathbf{G}_3$ are created by TTCT. Thereafter, by utilizing **sync**, the general specification $\mathbf{S}$ shown in Fig. 9(b) is generated.

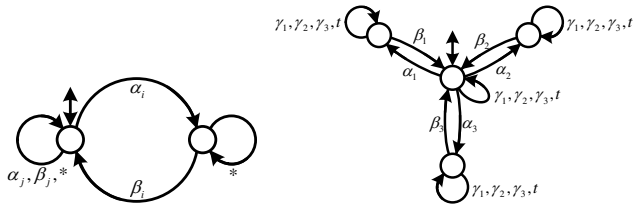

(a) τ_i (b) General Model

Fig. 9: Specification for CW real-time tasks.

B. Specification for MJGS Model

The initial preemptive specification for a JGS model is shown in Fig. 3 in [7]. In the present paper, it is revised to possess an initial and marker state, which is the specification of the MJGS model. The preemptive specification $\mathbf{S}_b$ for $\mathbf{G}_b$, represented by PRB, is created by TTCT. $\mathbf{S}_b$ is depicted in Fig. 10 with $* = \{t, a_a, a_b\}$.

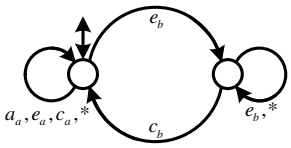

Fig. 10: MJGS model specification.

C. Dynamic Reconfiguration of RTS

For both CW and JGS models, the reconfiguration process is illustrated in Fig. 11, which is extended into a two-step approach. In the next section we will illustrate the supervisory control and reconfiguration of two real-world examples.

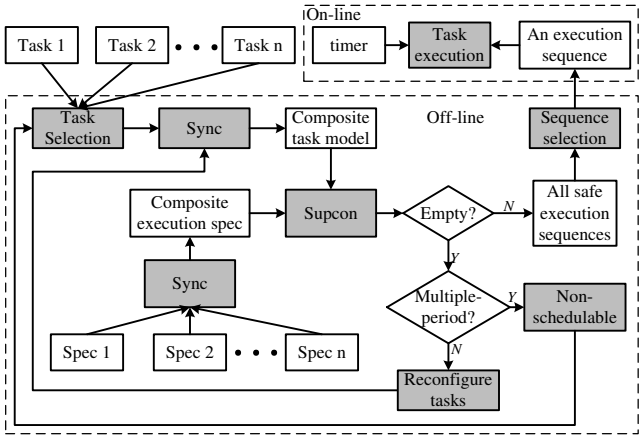

Fig. 11: Procedures for real-time scheduling.

Suppose that in every scheduling plan only a subset of tasks executed by an RTS enters the uni-processor for execution. Initially the tasks are running in the periodic version with lower bound $T_{i_{min}}$. Thus, the initial processor utilization of initial system $\mathbb{S}_0$ is $U_{max} = \sum_{i=1}^{n} C_i/T_{i_{min}}$. In case that $\mathbb{S}_0$ is non-schedulable, i.e., no safe execution sequence can be found by supervisory control, $\mathbb{S}_0$ should be reconfigured dynamically at run-time. All the tasks are replaced by the corresponding multiple-period TDES models with $T_i = [T_{i_{min}}, T_{i_{max}}]$, which is followed by supervisory control again to find all the safe execution sequences (possible reconfiguration scenarios). For any composite task model and the general specification, we find (using Theorem 1) all the safe execution sequences by **supcon**. For any task assigned with multiple-periods, its exact processor utilization lies between $U_{i_{min}}$ and $U_{i_{max}}$. Consequently, the processor utilization of the reconfigured RTS $\mathbb{S}$ lies between U_{min} and U_{max}, i.e.,

$$U_{min} \leq U_{\mathbb{S}} \leq U_{max}.$$

All possible safe execution sequences are found, resulting in a decrease of processor utilization. Users should take the responsibility to provide the lowest tolerable processor utilization U_{min}. Consequently, any safe execution sequence in the supervisor can be selected to schedule the RTS by dynamically reconfiguring the period of each task. If the supervisor is still empty, we claim that the system is non-schedulable.

VI. Examples

The reconfigurations are based on the revised versions of the two examples studied in [6] and [7], respectively.

A. Dynamic Reconfiguration of MCW Model

In this study, as illustrated in Fig. 12, the example of a motor network studied in [6] is revised and considered as a reconfigurable RTS. Suppose that three electric motors are controlled by a uni-processor. As depicted in Fig. 12, their deadlines and the periods are represented by D and T, respectively. At each time only a subset of these motors is called by the processor. Their parameters coincide with those of the tasks shown in Table II, i.e., τ_1 (Motor 1), τ_2 (Motor 2), and τ_3 (Motor 3). Suppose that the motor network has two work plans, coinciding with the defined RTS $\mathbb{S}^0$ and $\mathbb{S}^1$:

Plan 1. use only Motors 1 and 2; and

Plan 2. use all three motors.

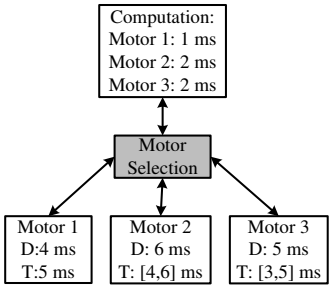

Fig. 12: A motor network example.

1) Supervisory Control of $\mathbb{S}_l^0$:

Take $\mathbb{S}_l^0$ (LSYS0) as an example. All the safe execution sequences are calculated by the procedure **supcon**, i.e.,

LSUPER0 = **supcon** (LSYS0, SPEC) (153, 190).

Since LSUPER0 is not empty, $\mathbb{S}_l^0$ is schedulable at utilization $U_{max} = 1/5 + 2/4 = 0.7$. The safe execution sequence set in LSUPER0 is represented by a TDES with 153 states and 190 transitions. By projecting out all events but α_i, i.e.,

PJLSUPER0 = **project** (LSUPER0, Image [11, 21]) (12, 15)

we obtain the scheduling map illustrated in Fig. 13, which contains 12 states and 15 transitions. PJLSUPER0 provides eight safe execution sequences to schedule the RTS with processor utilization being 0.7:

1. $\alpha_1\alpha_2\alpha_2\alpha_1\alpha_2\alpha_1\alpha_2\alpha_1\alpha_2$
2. $\alpha_1\alpha_2\alpha_2\alpha_1\alpha_2\alpha_1\alpha_2\alpha_2\alpha_1$
3. $\alpha_1\alpha_2\alpha_1\alpha_2\alpha_2\alpha_1\alpha_2\alpha_1\alpha_2$
4. $\alpha_1\alpha_2\alpha_1\alpha_2\alpha_2\alpha_1\alpha_2\alpha_2\alpha_1$
5. $\alpha_2\alpha_1\alpha_2\alpha_1\alpha_2\alpha_1\alpha_2\alpha_1\alpha_2$
6. $\alpha_2\alpha_1\alpha_2\alpha_1\alpha_2\alpha_1\alpha_2\alpha_2\alpha_1$
7. $\alpha_2\alpha_1\alpha_1\alpha_2\alpha_2\alpha_1\alpha_2\alpha_1\alpha_2$
8. $\alpha_2\alpha_1\alpha_1\alpha_2\alpha_2\alpha_1\alpha_2\alpha_2\alpha_1$

For comparison, the EDF scheduling result of $\mathbb{S}_l^0$ by Cheddar [27] is displayed in Fig. 14, which coincides with Sequence (1.) above within PJLSUPER0. Sequence (8.), depicted in Fig. 15, can never be generated by EDF. By comparing

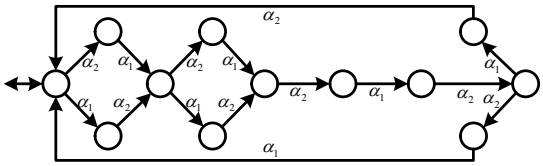

Fig. 13: Scheduling map of $\mathbb{S}_l^0$.

the two sequences in Figs. 14 and 15, in case τ_2^l (with the earliest deadline) cannot arrive on time at $t = 4$, then according to the multiple sequences users can choose another available sequence shown in Fig. 13 to schedule task τ_1 first. Thus, recalculating the scheduling sequences is unnecessary. However, there is no EDF sequence to schedule task τ_1 first. If τ_2 cannot arrive on time, the EDF scheduling cannot schedule $\mathbb{S}_l^0$ successfully. The supervisory control technique provides a greater number of safe execution sequences as compared to EDF scheduling.

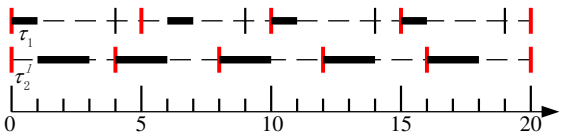

Fig. 14: Scheduling map of $\mathbb{S}_l^0$ in Cheddar.

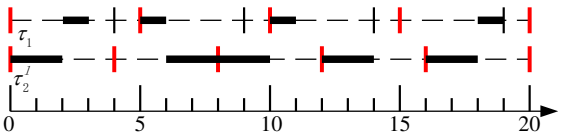

Fig. 15: Scheduling of Sequence (8.).

Intuitively, because $L(\mathbf{G}_2^l) \subset L(\mathbf{G}_2)$ and $L_m(\mathbf{G}_2^l) \subset L_m(\mathbf{G}_2)$, the safe execution sequences in $\mathbb{S}_l^0$ should be a proper subset of the safe execution sequences of $\mathbb{S}^0$. This is proved as follows. By calling procedure **supcon**, all the safe execution sequences of the multiple-period version RTS $\mathbb{S}^0$ are obtained. By using the procedure **complement**, we obtain the set of the behaviors prohibited by SUPER0, which is contained in CSUPER0. By computing the **meet** of CSUPER0 and LSUPER0, if the **trim** [25] version of **meet** is empty, this represents that the reachable and coreachable sequences within LSUPER0 are not in CSUPER0. Hence, LSUPER0 is a proper subset of SUPER0. The corresponding TTCT operations are

SUPER0 = **supcon** (SYS0, SPEC) (263, 362)

CSUPER0 = **complement** (SUPER0, []) (264, 1848)

TEST = **meet** (CSUPER0, LSUPER0) (156, 195)

TEST = **trim** (TEST) (0, 0)

The scheduling map for $\mathbb{S}^0$ is more complex than that for $\mathbb{S}_l^0$, which has 50 states and 86 transitions, i.e.,

PJSUPER0 = **project** (SUPER0, Image [11, 21]) (50, 86)

Evidently, even though the supervisor for $\mathbb{S}_l^0$ excludes some safe execution sequences of $\mathbb{S}^0$, the scheduling map still provides more choices than the EDF scheduling algorithm.

2) Dynamic Reconfiguration of $\mathbb{S}_l^1$:

The set of safe execution sequences of $\mathbb{S}_l^1$ (LSYS1) found by the procedure **supcon** is empty, i.e.,

LSUPER1 = **supcon** (LSYS1, SPEC) (0, 0)

According to the CW model, $\mathbb{S}_l^1$ is non-schedulable at processor utilization $U_{max} = 1/5 + 2/4 + 2/3 > 1$. Thus, we need to reconfigure the system to be the multiple-period model $\mathbb{S}^1$ (SYS1) and utilize SCT again to find the safe execution sequences by

SUPER1 = **supcon** (SYS1, SPEC) (2180, 3681)

This represents that **supcon** finds all the possible safe execution sequences between the processor utilization $U_{min} = 1/5 + 2/6 + 2/5 < 1$ and $U_{max} = 1/5 + 2/4 + 2/3 > 1$.

The system is finally schedulable since SUPER1 is nonempty. In order to find the scheduling map after the reconfiguration, we need to call **project**. However, TTCT fails to output the result of projecting onto events α_i. The reason is that the dynamic reconfiguration of the periods (event γ_i) violates the observer property discussed in [25]. However, we choose the following method to view a part of the scheduling map of the reconfigured RTS $\mathbb{S}^1$:

Step 1:

We choose $\mathbb{S}_u^1$ as a subset of the composite task model of $\mathbb{S}^1$, based on which we find the safe execution sequence set, containing 417 states and 574 transitions. The scheduling map is calculated by projecting the safe execution sequences onto events α_1, α_2, and α_3; it contains 37 states and 54 transitions, as seen in Fig. 16. The corresponding TTCT operations are given as follows.

USUPER1 = **supcon** (USYS1, SPEC) (417, 574)

PJUSUPER1 = **project** (USUPER1, Image [11, 21, 31]) (37, 54)

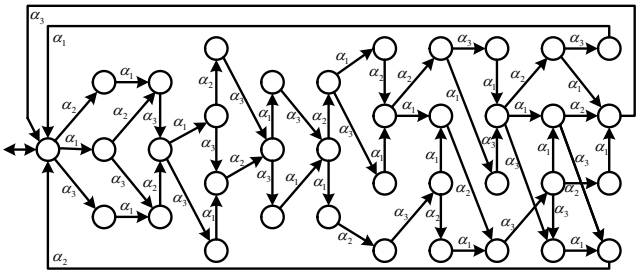

Fig. 16: Scheduling map of $\mathbb{S}_u^1$.

Step 2:

We can verify that $\mathbb{S}_u^1$ is a proper subset of $\mathbb{S}^1$ via the following TTCT procedures:

CSUPER1 = **complement** (SUPER1, []) (2181, 21810)

TEST = **meet** (CSUPER1, USUPER1) (417, 574)

TEST = **trim** (TEST) (0, 0)

Finally, we claim that, after the reconfiguration, the scheduling map of $\mathbb{S}^1$ is at least as complex as that presented in Fig. 16. More precisely, SUPER1 (resp., USUPER1) contains 2180 (resp., 417) states and 3681 (resp., 574) transitions. Intuitively, the scheduling map of SUPER1 should be more complex than that depicted in Fig. 16, in which the periods are dynamically reconfigured. The EDF scheduling of $\mathbb{S}_u^1$ by Cheddar is illustrated in Fig. 17. It can find only one schedulable sequence. Moreover, no sequence for the multiple-period RTS can be found by EDF scheduling in Cheddar.

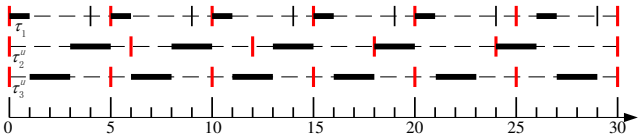

Fig. 17: Scheduling map of $\mathbb{S}_u^1$ in Cheddar.

3) Comparison with the CW model:

In LSUPER0 (CW model), every scheduling sequence is based on the fixed period of each task. The processor utilization of each task is fixed permanently. For example, we randomly choose a sequence $\gamma_1\alpha_1\gamma_2 t\beta_2 t\alpha_2 tt\beta_2\gamma_2\ldots$. By projecting out γ_1, α_1, and β_1, we obtain $\gamma_2 t\beta_2 t\alpha_2 tt\beta_2\gamma_2\ldots$. We have $T_2 = 4$ and $U_2 = 2/4$.

In SUPER0 (MCW model), we randomly choose two sequences as follows:

1. $\gamma_1\alpha_1\gamma_2 t\beta_1\alpha_2 tt\beta_2 tt\gamma_2\ldots$.
2. $\gamma_1\alpha_1\gamma_2 t\beta_1 tt\alpha_2 t\gamma_1 t\beta_2\gamma_2\alpha_2 tt\beta_2\alpha_1 t\beta_1 t\gamma_2\ldots$.

By projecting out γ_1, α_1, and β_1 in Sequence (1.), we obtain $\gamma_2 t\alpha_2 tt\beta_2 tt\gamma_2\ldots$. Obviously, we have $T_2 = 5$. The processor utilization of τ_2 is $2/5$.

By projecting out γ_1, α_1, and β_1 in Sequence (2.), we obtain $\gamma_2 ttt\alpha_2 tt\beta_2\gamma_2\alpha_2 tt\beta_2 tt\gamma_2\ldots$. Evidently, $T_2 = 5$ and $T_2 = 4$ are in two adjacent periods. In the second period of the execution of τ_2, its processor utilization is changed from $2/5$ to $2/4$ to speed up the scheduling process. This means that, according to the processor utilization interval predefined by the users, the processor utilization of the RTS is dynamically changed at run-time.

By comparing Sequences (1.) and (2.), we see that after the occurrence of substring $\gamma_1\alpha_1\gamma_2 t\beta_1$, the controller provides at least two subsequences in Sequences (1.) and (2.) to schedule τ_2. However, neither the CW scheduling nor the EDF scheduling can provide such scheduling plans.

4) Comparison with EDF real-time scheduling:

In this paper, for the real-time scheduling of each task, we require that its deadlines should be less than or equal to its period. Let $\tau_i = (R_i, C_i, D_i, T_i)$ be a task with multiple-period $T_i = [T_{i_{min}}, T_{i_{max}}]$. Let a period T satisfy $T_{i_{min}} \leq T \leq T_{i_{max}}$. The execution of τ_i should be finished no later than $\min\{D_i, T\}$. According to the EDF scheduling algorithm, the shortest period $T = T_{i_{min}}$ assigns the task the highest priority. In this case, suppose that we have a periodic RTS $\mathbb{S}^2 = \{\tau_1, \tau_2, \tau_3\}$ with $\tau_1 = (0, 2, 8, [6, 8])$, $\tau_2 = (0, 2, 10, [7, 10])$, and $\tau_3 = (0, 4, 7, 8)$. As illustrated in Fig. 18, task τ_3 finishes its execution at time $t = 8$, which misses its deadline $D_3 = 7$. The EDF scheduling of $\mathbb{S}^2$ is non-schedulable. However, according to the developed reconfiguration technique, we obtain a supervisor with 2854 states and 4287 transitions. Thus we claim that, $\mathbb{S}^2$ is schedulable under the presented scheduling algorithm.

B. Dynamic Reconfiguration of MJGS model

1) Dynamic Reconfiguration of $\mathbb{S}_l^J$:

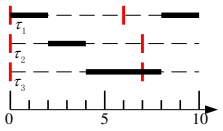

Fig. 18: EDF scheduling map of $\mathbb{S}$.

Consider a water vessel system [7] represented by two tasks as listed in Table III. The first task τ_a is assigned with a multiple-period $[2, 3]$. The RTS cannot be scheduled according to the initial plan with processor utilization $U_{max} = 1/2 + 2/3 \geq 1$, i.e.,

LJ = **trim** (LJ) (0, 0)

The full scheduling map of $\mathbb{S}_l^J$ is empty, which means that the system represented by the JGS model is non-schedulable. In order to reconfigure $\mathbb{S}_l^J$, τ_a^l is revised to be τ_a with a multiple-period. Then we obtain the full schedule map shown in Fig. 19 by

J = **trim** (J) (15, 29)

J = **project** (J, Null [11]) (13, 16)

During the reconfiguration, $T_a = 3$ is selected automatically. The processor utilization is $U_{min} = 1/3 + 2/3 = 1$ and thus the RTS is schedulable. According to [7], by assigning higher priorities for task τ_a and τ_b, we obtain the safe execution sequences shown in Figs. 20 and 21, respectively.

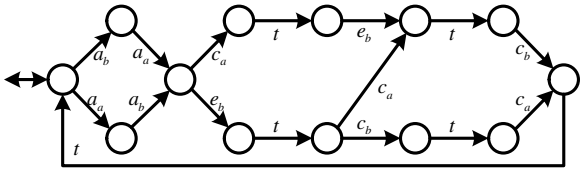

Fig. 19: The full scheduling map.

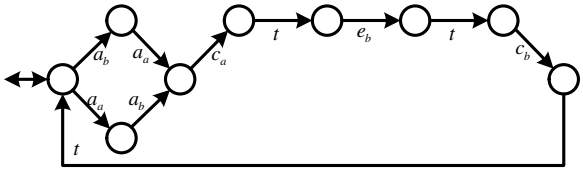

Fig. 20: Task τ_a with a higher priority.

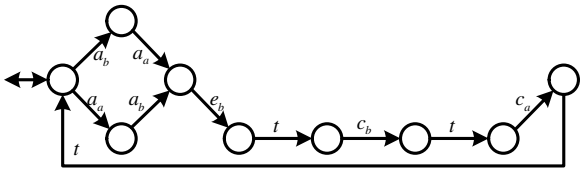

Fig. 21: Task τ_b with a higher priority.

If we only use the non-preemptive specification, without considering the priorities to calculate the controller, i.e.,

SUPER = **supcon** (J, PRB) (13, 15)

we obtain the scheduling map as shown in Fig. 22.

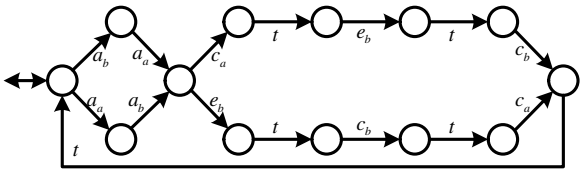

Fig. 22: Non-preemptive scheduling.

2) Comparison with the JGS model:

Suppose that the initial period of τ_a is $T_a = 3$. The system is schedulable based on the technique proposed in [7]. However, the real time scheduling in [7] is priority-based. Thereafter, the non-preemptive scheduling can be based only on the scheduling map shown in Fig. 20 or 21. In that case the scheduling shown in Fig. 22 can never be found. Obviously, the real-time scheduling in this paper is more general.

VII. Discussion

A. Computational Complexity

The real-time scheduling and reconfiguration are based on the computation of the supremal controllable sublanguage with respect to a finite TDES. According to [6] and [28], the computation of the supremal controllable sublanguage with respect to a finite TDES can be completed in polynomial time. Similar to [6], the computational complexity of the presented method in this study is characterized by 1) the modeling of a processor time unit as a distinct event in the DES framework and 2) the exponential growth with respect to the number of states when synchronous product is utilized to combine individual tasks into the plant. The computational complexity of the supremal sublanguage of a specification is $O(m^2n^2)$ where m and n are the size of the final state set of the plant $\mathbf{G}$ and the specification $\mathbf{S}$, respectively.

In this work, the increase of a period is obtained by explicitly adding the *tick* event. If an RTS executes a large set of periodic tasks that are assigned with large periods, then the number of states and transitions will be increased significantly. Similar to [6], this remains a challenge in the "scaling up" of the proposed method for the reconfiguration based on SCT. Two approaches may be explored to deal with this difficulty. One approach, namely modular synthesis [29], may be applied to reduce computational overload by synthesizing a set of modular supervisors which can achieve the same result as a centralized supervisor does. Another approach is to use supervisory control of the timed version of state-tree-structures [30] to manage the state explosion problem in the calculation of the supervisors.

B. Calculation of Supremal Controller

Instead of on-line monitoring, we calculate the supervisor off-line, which has both advantages and disadvantages. On the one hand, since the supervisor is supremal and contains all the safe execution sequences, it is possible that during the real-time scheduling, users do not have to be concerned with the tasks' parameters. By only following any sequence in the supervisor, users can schedule/reconfigure an RTS.

The verification time of event enabling/disabling is linear with respect to the number of the supervisor's states. On the other hand, the state size of the supervisor may increase exponentially with the number of tasks. The two possible approaches in Section VII-A to solve the "scaling up" problem may also confront this challenge.

In comparison, the on-line monitoring also has an advantage and some disadvantages. The advantage is that users can just follow the monitor to schedule the RTS. However, the disadvantages are that the on-line monitoring may fail to schedule the RTS, and the computational complexity of finding the scheduler is higher than the complexity of the supremal SCT controller verification.

C. Comparison with Other Reconfiguration Methods

Job skipping can be utilized by an RTS to execute "occasionally skippable" tasks, such as video reception, telecommunications, packet communication, and aircraft control [19]. However, industrial production lines should avoid job skipping since it will increase the manufacturing cost. As another approach, the elastic scheduling model [8]–[11] can be utilized to guarantee that no deadline is missed during the manufacturing process in industrial applications [31]. However, both reconfiguration approaches can only provide a single sequence on-line. Moreover, even though all the deadlines are satisfied by the elastic scheduling model, the processor utilization of some tasks is decreased.

For industrial production lines or manufacturing processes, the technique presented in this study reconfigures an RTS that executes a set of tasks with the same task scale studied in [6]–[11]. We suggest that users predefine an acceptable processor utilization interval for each task. If no safe execution sequence can be found at the highest processor utilization, SCT is utilized to provide all the possible safe execution sequences by off-line supervisory control.

Both job skipping and the elastic task model need to calculate the processor demand. However, the method provided in this study does not need to calculate the processor demand. The comparison is shown in Table V.

TABLE V: Comparison with other reconfiguration methods

method	on-line	single sequence	processor demand
job skipping	Y	Y	Y
elastic task	Y	Y	Y
this work	N	N	N

VIII. Conclusion

This study presents a formal constructive method for real-time periodic tasks with multiple-periods via a TDES model. The lower and upper bounds of the period of such a model are predefined by users for the purpose of dynamic reconfiguration. The formal SCT of TDES can be considered as a rigorous analysis and synthesis tool to dynamically reconfigure the non-preemptive scheduling of hard RTS. Suppose that in every scheduling plan only a subset of tasks of an RTS is called by the processor. Instead of dynamically updating the specification for the tasks running in the uni-processor, a general specification is presented, which guarantees that all the potential tasks called by the processor can be scheduled non-preemptively. In case an RTS is claimed by [6] or [7] to be non-schedulable, the presented two-step dynamic reconfiguration approach can be utilized to find all the safe execution sequences (possible reconfiguration scenarios) of each task in the RTS. These sequences provide more choices than the EDF scheduling algorithm. The processor and the real-time tasks are general models for real-world hard RTS. Similar to [6] and [7], the multiple-period model can be utilized to describe the behavior of a manual assembly process or a robotic pick-and-place operation that is executed by a processor that could be a water vessel system, computer numerical control (CNC) machine, a robot, or an assembly-line worker. This leads to the possibility that the off-line reconfiguration method can be implemented in practical contexts based on reconfigurable real-time scheduling. In future work, we will focus on the dynamic reconfiguration of RTS processing asynchronous tasks and sporadic tasks. The real-time scheduling can be preemptive or non-preemptive.

References

[1] C. L. Liu and J. W. Layland, "Scheduling algorithms for multiprogramming in a hard real time environment," *J. Assoc. Comput. Mach.*, vol. 20, no. 1, pp. 46–61, 1973.

[2] E. Nassor, and G. Bres, "Hard real-time sporadic task scheduling for fixed priority schedulers", in *Proc. intern. workshop on responsive syst.*, pp. 44–47, 1991.

[3] G. Buttazzo, M. Bertogna, and G. Yao, "Limited preemptive scheduling for real-time systems: A survey," *IEEE Trans. Ind. Inform.*, vol. 9, no. 1, pp. 3–15, 2013.

[4] L. Lo Bello, E. Bini, G. Patti, "Priority-driven swapping-based scheduling of aperiodic real-time messages over etherCAT networks," *IEEE Trans. Ind. Inform.*, vol. 11, no. 3, pp. 741-751, 2015.

[5] N. Q. Wu, M. C. Zhou, and Z.W. Li, "Short-term scheduling of crude-oil operations: Petri net-based control-theoretic approach," *IEEE Robot Autom. Mag.*, vol. 22, no. 2, pp. 64–76, 2015.

[6] P. C. Y. Chen and W. M. Wonham, "Real-time supervisory control of a processor for non-preemptive execution of periodic tasks," *Real-Time Syst.*, vol. 23, pp. 183–208, 2002.

[7] V. Janarthanan, P. Gohari, and A. Saffar, "Formalizing real-time scheduling using priority-based supervisory control of discrete-event systems", *IEEE Trans. Autom. Cont.*, vol. 51, no. 6, pp. 1053–1058, 2006.

[8] G. Buttazzo, G. Lipari, and L. Abeni, "Elastic task model for adaptive rate control," in *Proc. 19th Real-Time Syst. Symp.*, 1998, pp. 286–295.

[9] G. Buttazzo and L. Abeni, "Adaptive workload management through elastic scheduling," *Real-Time Syst.*, vol. 23, no. 1–2, pp. 7–24, 2002.

[10] G. Buttazzo, G. Lipari, M. Caccamo, and L. Abeni, "Elastic scheduling for flexible workload management", *IEEE Trans. Comput.*, vol. 51, no. 3, pp. 289–302, 2002.

[11] M. Marinoni and G. Buttazzo, "Elastic DVS management in processors with discrete voltage/frequency modes," *IEEE Trans. Ind. Inform.*, vol. 3, no. 1, pp. 51–62, 2007.

[12] L. Sha, T. Abdelzaher, K. E. Årzén, A. Cervin, T. Baker, A. Burns, G. Buttazzo, M. Caccamo, J. Lehoczky, and A. K. Mok, "Real time scheduling theory: A historical perspective," *Real-Time Syst.*, vol. 28, no. 2, pp. 101–155, 2004.

[13] X. Wang, I. Khemaissia, M. Khalgui, Z. W. Li, O. Mosbahi, and M. C. Zhou, "Dynamic low-power reconfiguration of real-time systems with periodic and probabilistic tasks," *IEEE Trans. Autom. Sci. Eng.*, vol. 12, no. 1, pp. 258–271, 2015.

[14] J. Cecilio and P. Furtado, "Architecture for uniform (re)configuration and processing over embedded sensor and actuator networks," *IEEE Trans. Ind. Inf.*, vol. 10, no. 1, pp. 53–60, 2014.

[15] M. Garcia-Valls, I. R. López, and L. F. Villar, "iLAND: An enhanced middleware for real-time reconfiguration of service oriented distributed real-time systems," *IEEE Trans. Ind. Inf.*, vol. 9, no. 1, pp. 228–236, 2013.

[16] L. Li, S. Li, and S. Zhao, "QoS-aware scheduling of services-oriented internet of things," *IEEE Trans. Ind. Inf.*, vol. 10, no. 2, pp. 1497–1505, 2014.

[17] M. N. Rooker, C. Sünder, T. Strasser, A. Zoitl, O. Hummer, and G. Ebenhofer, "Zero downtime reconfiguration of distributed automation systems: The εCEDAC approach," in *Proc. Int. Conf. Indust. Appl. Holonic Multi-Agent Syst.*, Regensburg, Sept. 2007, pp. 326–337.

[18] P. Vrba and V. Marik, "Capabilities of dynamic reconfiguration of multiagent-based industrial control systems", *IEEE Trans. Syst. Man Cybern., Part A: Syst. Humans*, vol. 40, no. 2, pp. 213–223, 2010.

[19] G. Koren and D. Shasha, "Skip-over: Algorithms and complexity for overloaded systems that allow skips," in *Proc. 19th Real-Time Syst. Symp.*, pp. 110–117, 1995.

[20] L. George, and P. Courbin, "Reconfiguration of uniprocessor sporadic real-time systems: the sensitivity approach," *book chapter in IGI-Global Knowledge on Reconfigurable Embedded Control Systems: Applications for Flexibility and Agility*, Hershey, PA, USA: IGI Global, 2011, pp. 167–189.

[21] L. B. Lo, E. Bini, and G. Patti, "Priority-driven swapping-based scheduling of aperiodic real-time messages over EtherCAT networks," *IEEE Trans. Ind. Inform.*, vol. 11, no. 3, pp. 741–751, 2015.

[22] A. Kavousi-Fard, M. A. Rostami, and T. Niknam, "Reliability-oriented reconfiguration of vehicle-to-grid networks," *IEEE Trans. Ind. Inform.*, vol. 11, no. 3, pp. 682–691, 2015.

[23] S. Baruah, R. Howell, and L. Rosier, "Algorithms and complexity concerning the preemptive scheduling of periodic real-time tasks on one processor," *Real-Time Syst.*, vol. 2, pp. 301–324, 1990.

[24] P. J. Ramadge and W. M. Wonham, "Supervisory control of a class of discrete event processes," *SIAM J. Contr. Optim.*, vol. 25, no. 1, pp. 206–230, 1987.

[25] W. M. Wonham, *Supervisory control of discrete-event systems*, Department of Electrical and Computer Engineering, University of Toronto, 2015. Available at http://www.control.utoronto.ca/DES.

[26] B. Brandin and W. M. Wonham, "Supervisory control of timed discrete event systems," *IEEE Trans. Autom. Cont.*, vol. 39, no. 2, pp. 329–342, 1994.

[27] F. Singhoff, J. Legrand, L. Nana, and L. Marce, "Cheddar: A flexible real time scheduling framework," in *Proc. Int. ACM SIGAda Conf.*, pp. 1–8, 2004.

[28] P. J. Ramadge and W. M. Wonham, "The control of discrete event systems," *Proceedings of the IEEE*, vol. 77, no.1, pp. 81–98, 1989.

[29] W. M. Wonham and P. J. Ramadge, "Modular supervisory control of discrete event systems," *Math. of Cont. Signal Syst.*, vol. 1, no. 1, pp. 13–30, 1988.

[30] C. Ma and W. M. Wonham, *Nonblocking Supervisory Control of State Tree Structures*, Lecture Notes in Control and Information Sciences (LNCIS) 317, Springer, 2005.

[31] A. Girbea, C. Suciu, S. Nechifor, and F. Sisak, "Design and implementation of a service-oriented architecture for the optimization of industrial applications," *IEEE Trans. Ind. Inform.*, vol. 10, no. 1, pp. 185–196, 2014.

Xi Wang received the B.S. degree in Automation from Liren College, Yanshan University, Qinhuangdao, China, in 2008 and the M.S. degree in Mechanical-Electronic Engineering from Xidian University, Xi'an, China, in 2011. He is working toward the Ph.D degree in the School of Electro-Mechanical Engineering, Xidian University, Xi'an, China. Also, he is currently a visiting PhD student at the Systems Control Group, Department of Electrical and Computer Engineering, University of Toronto, Canada. His research interests include dynamic reconfiguration of real-time scheduling and supervisory control of discrete-event systems.

ZhiWu Li (M'06–SM'07) received the B.S., M.S., and Ph.D. degrees in mechanical engineering, automatic control, and manufacturing engineering, respectively, all from Xidian University, Xi'an, China, in 1989, 1992, and 1995, respectively. He joined Xidian University in 1992 and now he is also with the Institute of Systems Engineering, Macau University of Science and Technology, Taipa, Macau. Over the past decade, he was a Visiting Professor at the University of Toronto, Technion–Israel Institute of Technology, Martin-Luther University of Halle–Wittenburg, Conservatoire National des Arts et Métiers (CNAM), Meliksah Universitesi. His current research interests include Petri net theory and application, supervisory control of discrete event systems, workflow modeling and analysis, system reconfiguration, game theory, and data and process mining. He is a member of Discrete Event Systems Technical Committee of the IEEE Systems, Man, and Cybernetics Society, and a member of IFAC Technical Committee on Discrete Event and Hybrid Systems from 2011 to 2014. He serves as a frequent reviewer for 50+ international journals including Automatica and a number of the IEEE Transactions as well as many international conferences. He is listed in Marquis Who's Who in the world, 27th Edition, 2010. Dr. Li is a recipient of an Alexander von Humboldt Research Grant, Alexander von Humboldt Foundation, Germany. He is a senior member of IEEE and is the founding chair of Xi'an Chapter of IEEE Systems, Man, and Cybernetics Society.

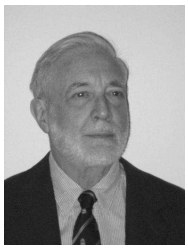

W. M. Wonham (M'64–SM'76–F'77–LF'00) received the B.Eng. degree in engineering physics from McGill University, Montreal, QC, Canada, in 1956, and the Ph.D. degree in control engineering from the University of Cambridge, Cambridge, U.K., in 1961. From 1961 to 1969, he was associated with several U.S. research groups in control. Since 1970, he has been a faculty member in systems control, with the Department of Electrical and Computer Engineering, University of Toronto. His research interests have included stochastic control and filtering, geometric multivariable control, and discrete-event systems. He is the author of Linear Multivariable Control: A Geometric Approach (Springer-Verlag, 3rd ed., 1985), coauthor (with C. Ma) of Nonblocking Supervisory Control of State Tree Structures (Springer-Verlag, 2005), and coauthor (with K. Cai) of Supervisor Localization: A Top-Down Approach to Distributed Control of Discrete-Event Systems (Springer-Verlag, 2015). Dr. Wonham is a Fellow of the Royal Society of Canada, a Life Fellow of the IEEE, a Foreign Member of the (U.S.) National Academy of Engineering, and Honorary Professor of the Beijing Institute of Aeronautics and Astronautics. In 1987 he received the IEEE Control Systems Science and Engineering Award and in 1990 was Brouwer Medallist of the Netherlands Mathematical Society. In 1996 he was appointed University Professor in the University of Toronto, and in 2000 University Professor Emeritus.